Nuclear Inst. and Methods in Physics Research, A 928 (2019) 43–50

Contents lists available at ScienceDirect

Nuclear Inst. and Methods in Physics Research, A

journal homepage: www.elsevier.com/locate/nima

Practical considerations in modeling the low light response of photomultiplier tubes in large batch testing

D. Coquelin, T. Jobin, W. Kemmerer, P. Maxwell, S. Merten, E. Moller, W. Morris, G. Niculescu *, I. Niculescu, W. Shaver

James Madison University, Harrisonburg, VA 22807, United States

ARTICLE INFO

Keywords:
Photomultiplier
Single photoelectron response
Cherenkov
Machine learning
Artificial neural network

ABSTRACT

Photomultiplier tubes continue to be a reliable, cost-effective means of detecting light produced by the interaction of subatomic particles with detectors. For detectors where the expected light yield is modest, characterizing the low light response of the tube is of paramount importance. Several phenomenological models addressing this issue exist. This paper presents side-by-side comparison between three such approaches as they arose from a large scale testing of tubes to be used by a Ring Imaging Cherenkov detector at Jefferson Lab. The main characteristics of the tubes, such as the gain, were found to be consistent within the expected uncertainties for all models considered. Leveraging the extensive nature of the study, a machine learning algorithm based on an artificial neural network capable of obtaining the tube characteristics directly from the raw ADC data was developed and trained. The trained neural network produced results fully compatible with the three models considered, with substantial savings in both computation time and experimenter overhead.

1. Introduction

Photomultiplier Tubes (PMTs) have a long history of reliable service in nuclear and particle physics experiments, as well as other fields that require precise light detection (astronomy, nuclear medicine, defense). More modern alternatives, such as avalanche photodiodes, for light detection do exist; however, PMTs exhibit several desirable characteristics such as large potential gains, good gain stability, radiation hardness, long life expectancy. These properties, combined with the cost effectiveness in covering large detection areas will ensure their continuous usage in current and future experimental setups.

The data presented in this work stems from the more than 1000 PMTs tested in the Nuclear and Particle Physics Laboratory at James Madison University (JMU-PNP) for the Gas Ring Imaging Cherenkov (GRINCH) detector [1] in the experimental Hall A at the Thomas Jefferson National Accelerator Facility (JLab). To minimize the cost of the detector GRINCH has cylindrical mirrors that project the Čerenkov light onto a large (500+) array of 28.2 mm ET Enterprises 9125FLB17 PMTs. These were recovered from BABAR's DIRC [2] detector ("Detection of Internally Reflected Cherenkov light").

As with any Cherenkov detector the anticipated light level in GRINCH is very low (on average seven photoelectrons (p.e.) per event), thus the one photoelectron response, the gain and its stability, as well as the dark current were studied in detail as part of these tests. Furthermore, because these were reclaimed PMTs, extensive testing and selection from a larger pool of tubes was required.

This paper is structured as follows. In Section 2 we briefly describe the test stand and the testing protocol used for this study. Section 3 introduces the three phenomenologic parameterizations used to model the low light response of a PMT. Section 4 details the PMT characteristics relevant for this study and describes the data analysis procedure. The results from the three models are compared in Section 5. Considerations specific to large scale PMT testing are given in Section 6, including the development of a Machine Learning technique that can aid in analyzing such data. The last section presents our conclusions.

2. Test stand

The test stand designed and built in the Nuclear and Particle Physics Laboratory at JMU was optimized to study the PMT characteristics relevant to low light environment operation:

- the position of the pedestal and its stability with respect to the high voltage.
- the position of the one photoelectron peak.
- the peak-to-valley ratio for the one photoelectron peak.
- the PMT gain and its dependence on the high voltage.

* Corresponding author.
E-mail address: gabriel@jlab.org (G. Niculescu).

https://doi.org/10.1016/j.nima.2019.03.001
Received 16 January 2019; Received in revised form 21 February 2019; Accepted 3 March 2019
Available online 12 March 2019
0168-9002/

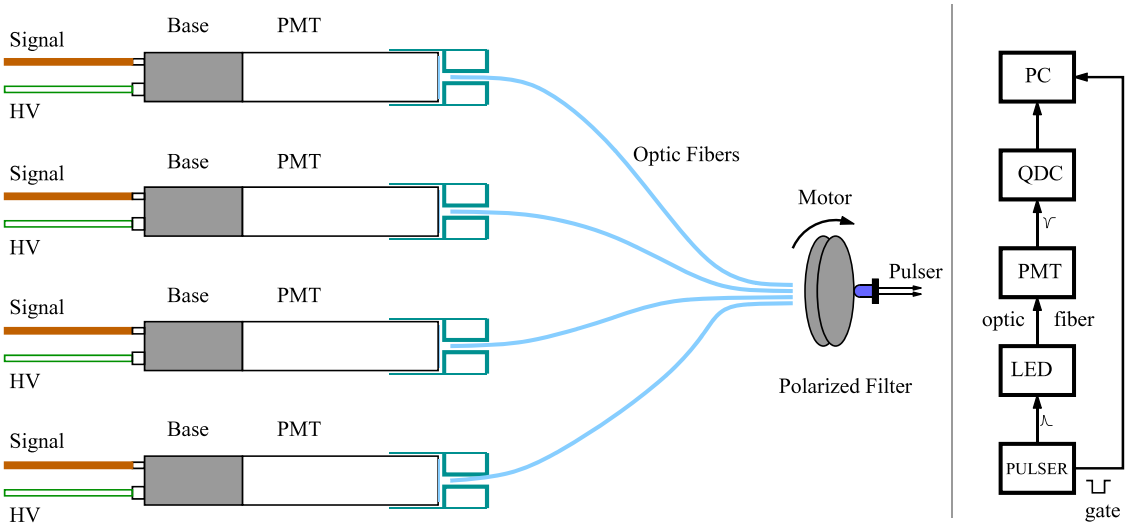

Fig. 1. Test stand layout: Mechanical and Electronic Layout for the PMT test stand used for the current study. Left: Schematic of the PMT test stand built and operated at JMU. The test stand could accommodate seven PMTs at a time, only four are shown here. Right: Logical scheme for testing one PMT.

- the Dark Current.

The meaning of most of these parameters follows the definitions from the Photomultiplier Handbook [3]. The peak-to-valley ratio was defined as the height of the one photoelectron peak divided by the height of the minimum (valley) between the pedestal and the one photoelectron peak. During the analysis this provided a convenient way of identifying and eliminating tubes that did not show a clear pedestal to one photoelectron peak separation. In this work the dark current was defined as the count rate above 0.25 photoelectrons in the absence of the light signal. All measured ADC spectra and relevant fit results and extracted parameters were saved in a ROOT [4] file to facilitate subsequent analysis (rejecting tubes, sorting tubes, etc.).

The right side of Fig. 1 shows the logical diagram for testing one PMT. An AVTEC AVP-AV-1-C pulse generator operating at 500–1000 Hz was used to pulse a blue LED with a peak emission wavelength of 460 nm, in the range of the expected Cherenkov radiation the PMTs are expected to detect. The width of each pulse was 2 ns. The PMT signals were digitized using a CAEN 16 Channel dual range QDC (V965) and were recorded using a VME-based data acquisition system running CODA, the JLab-developed data acquisition software [5]. For each PMT ADC spectra were recorded both on the 25 fC/channel and on the coarser 200 fC/channel QDC settings.

The setup was designed to accommodate the testing of several PMTs in parallel. The light signal from the LED was split into a bundle of seven optic fibers. Each fiber was fed into a custom 3D-printed cap that fits over the face of the PMT, as shown on the left hand side of Fig. 1.

To reduce the light level a low-cost (840 steps/rotation), remotely controlled polarized filter consisting of two linear filters rotating with respect to one another was built and inserted between the LED and the optic fiber bundle, as shown in Fig. 1. The reliability of the filter was tested by measuring the response of a single PMT using various filter settings (i.e. different readings of the motor encoder). Fig. 2 shows ADC spectra from this PMT for six light levels corresponding to average number of photoelectrons between 0.02 and 0.65, as obtained from a fit of the ADC data to the Bellami et al. model described below. As shown, the calculated gain of the PMT is very stable (at the 5% level) for all light levels tested. Based on this finding the filter level for the bulk testing was set such that ~90% of the triggers are pedestal events.

After being installed in the dark box (and every time thereafter when the dark box was opened) the PMTs were conditioned, with the high voltage turned on, for an hour before starting the data acquisition. The typical testing sequence for a batch of PMTs involved recording ADC spectra with the LED pulsed at 500–1000 Hz for several high

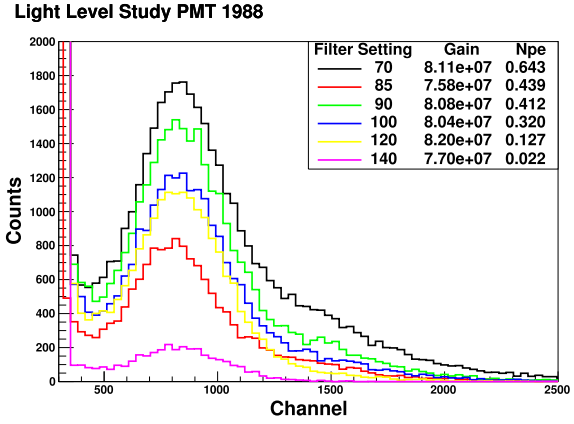

Fig. 2. Light source reliability testing: ADC spectra for PMT number 1988 for six different filter settings.

voltage settings (800–1400 V). The dark current run was taken at 1200 V. The running time was 5–10 min for the light pulsing runs and at least an hour for the dark current measurements.

3. Modeling the PMT response to low light levels

The low light response of photomultiplier tubes has been investigated extensively and several parameterizations have been developed. All of these studies make certain assumptions about the underlying physical phenomena associated with the conversion of the light signal into an electrical signal and its subsequent amplification and are thus able to model the phototube's response to light. The parameters of these models are obtained by fitting the PMT signal and they can be used to evaluate the relevant characteristics of the PMT. This section is a brief overview of the models used in this study [6–8].

3.1. The Dossi et al. model

In developing the ideal Single Electron Response (SER) of a PMT to a low light source this model assumes that the dark noise differs significantly from the (low) light signal and therefore cannot be used for calibration. Multiple photon emission and dynode noise further complicate the extraction of the ideal SER.

The ideal SER quoted in [6] is a sum of a Gaussian and an exponential:

$$SER_0(x) = \begin{cases} \frac{p_E}{A} e^{-\frac{x-x_p}{A}} + \frac{1}{\sigma_0\sqrt{2\pi}} \frac{1-p_E}{g_N} e^{-\frac{(x-x_0-x_p)^2}{2\sigma_0^2}}, & x > 0 \\ 0, & x \le 0 \end{cases} \quad (1)$$

where A is the slope of the exponential part of the SER, p_E is the fraction of events under the exponential, x_p is the pedestal position, x_0 and σ_0 are the mean value and the standard deviation of the Gaussian part of the single p.e. response, respectively. The factor g_N compensates for the usage of a truncated Gaussian.

$$g_N = \frac{1}{2}\left[1 + Erf\left(\frac{x_0}{\sqrt{2}\sigma_0}\right)\right] \quad (2)$$

The observed PMT response is the convolution of the ideal SER_0 with (Gaussian) noise:

$$SER(x) = SER_0(x) \otimes Noise(x) \quad (3)$$

Even for low light intensity the observed PMT response contains a component stemming from multiple primary p.e. Assuming a linear PMT response and taking into account the Poisson distribution (and its Gaussian approximation for the case when the number of photoelectrons is larger than 2), the multi photoelectron response is modeled in [6] as:

$$M(x) = \sum_{n=2}^{N_M} \frac{P(n;\mu)}{\sqrt{2n\pi}\sigma_1} e^{-\frac{1}{2n}(\frac{x-nx_1-x_p}{\sigma_1})^2} \quad (4)$$

Here μ is the expected (or average) number of photoelectrons per LED pulse.

3.2. The Bellamy et al. model

This model [7] treats the PMT as an instrument consisting of two independent parts: the photon detection system, responsible for converting (a part of) the incoming photon flux into electrons and the dynode-based amplifier system — which amplifies the initial charge produced by the photocathode.

The model assumes that the PMT response to a single photoelectron can be approximated by a Gaussian and that multiple photon emissions can be treated independently. The ideal SER is then a convolution between the multielectron Gaussian and the corresponding Poisson distribution.

$$SER_0(x) = P(n;\mu) \otimes G_n(x) \quad (5)$$

with $P(n;\mu)$ the Poisson probability distribution function and

$$G_n(x) = \frac{1}{\sigma_1\sqrt{2\pi n}} e^{-\frac{(x-nQ_1)^2}{2n\sigma_1^2}} \quad (6)$$

with Q_1 the average PMT charge for one photoelectron collected at the first dynode, σ_1 the standard deviation of the charge distribution, and n the number of photoelectrons collected.

The background processes are modeled as either a Gaussian (low charge processes present in all events such as leakage current) or as an exponential function (for discrete processes such as thermal emission). The "realistic" PMT spectrum is then obtained as a convolution between the ideal SER and the background processes.

3.3. The Degtiarenko model

In this more recent paper [8] the author develops a new method for describing the PMT response by taking into account the discrete statistical behavior of the electron cascade as well as allowing for non-uniformities in the gain structure of the first dynode. The spread induced by the second (and subsequent) dynode(s) is taken into account as well. This approach was used to successfully describe the performance of several types of photomultiplier tubes. According to this model, the normalized experimental PMT distribution can be approximated as:

$$f(a;\boldsymbol{d}) = \sum_{n=0}^{\infty} G(a,n;\sigma_{eff})\left[e^{-\mu} q_0(n) + \sum_{m=1}^{\infty} P(m;\mu) T(n,m;\boldsymbol{t})\right] \quad (7)$$

where a is the pedestal subtracted, normalized signal amplitude (normalized with respect to the model parameter **scale**), $\boldsymbol{d}$ includes the model variables $scale$, σ, μ and ξ, $\boldsymbol{t}$ includes the model variables ν_1, ν_2, ν_3, α_2, and α_3. A more detailed list of definitions and physical interpretation of the various quantities appearing in Eq. (7) can be found in [8]. Given the highly convoluted nature of the model the Ref. [8] advocates fitting the experimental data in stages, with various combinations of parameters being restricted/fixed while other parameters are allowed to vary. While this procedure does work, it tends to add a substantial amount of computer and/or experimenter overhead.

4. Data analysis

The raw data acquired was processed using a JMU-PNP-developed C++/ROOT-based program that converted the data into ROOT trees and filled various ADC histograms. To determine the parameters listed earlier the position of the pedestal and the one photoelectron peak have to be determined.

Gain Calculation.

For PMTs operating at relatively large light levels (several photoelectrons) the gain can be calculated from the width and position of the peak signal in the ADC distribution [9]. This approach relies on the fact that at large number of photoelectrons the Poisson distribution can be approximated with a Gaussian. The GRINCH PMTs however are expected to operate at very low light levels. In such an environment one needs to carefully model the PMT response in order to obtain the position of the pedestal and of the one photoelectron peak. As highlighted in the previous section several papers [6–8] describe the PMT response to low light intensity levels, providing sophisticated fitting functions/parameterizations.

For this study methods corresponding to these models were implemented in the PMT class defined in the C++ analysis. These functions were then used to fit the ADC spectra to obtain the position of the pedestal and of the first photoelectron peak, based on which the PMT gain can be calculated. A typical result of such a fitting procedure is shown in Fig. 3. For this particular run the light level was adjusted, using the polarized filter, to a level (~1.3 p.e.) where the contributions from two/more photoelectrons cannot be ignored. These contributions are depicted using the dashed curves in Fig. 3. In the code the fit parameters are named using the same convention as the original paper for all three models considered. For the Bellamy et al. model Q_1 is proportional to the tube gain.

High voltage dependence of gain.

The gain for each tube was measured at several high voltages (typically five settings) in the range 800 to 1400 V. The PMT response was then fitted to the three models described earlier.

For each high voltage setting the fit parameters for each model and their uncertainties were saved in a database indexed with the PMT number. For each tube the gain was plotted as a function of the applied high voltage and fitted with a simple exponential, as shown in Fig. 4:

$$G = A \ \ HV^{\gamma} \quad (8)$$

The A and γ coefficients shown in Fig. 4 are valid if the high voltage in Eq. (8) is expressed in kV, otherwise the fit suffers from severe instabilities due to the A term becoming very small.[1]

Dark Current.

[1] Alternatively one can try the more robust functional form $G = e^{p_0+p_1 HV}$. Generally the HV^{γ} form is preferred as the γ factor can be related to the number of PMT dinodes.

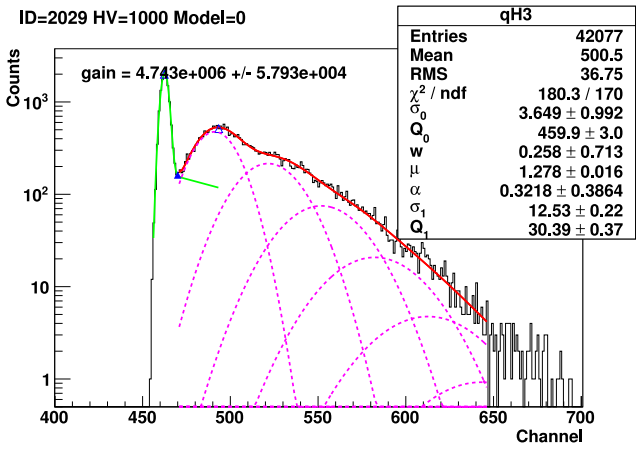

Fig. 3. PMT response fitting using the Bellamy et al. model for PMT # 2029 at 1000 V. The naming of the parameters matches the convention used in [7].

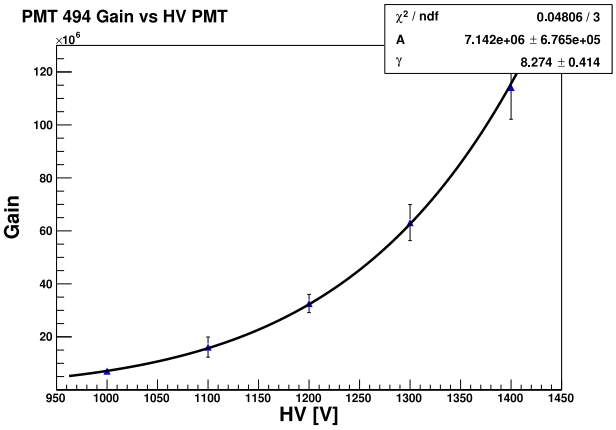

Fig. 4. Gain vs high voltage: PMT gain as a function of the applied High Voltage for tube # 494, together with an exponential fit of the measured gain.

Another parameter of interest for photomultiplier tubes expected to operate in low light environments is "dark current" (also known as "dark noise", "dark count", etc.),[2] i.e. the response of the PMT in the **absence** of any light signal. For an in-depth discussion of the possible sources of this effect see for example [3].

In the present study the dark count rate was measured at a high voltage setting of 1200 V, which is in the middle of the operating range for the 9125FLB17 PMTs. With the light source turned off each tube was conditioned under high voltage for at least one hour prior to taking an hour-long data run. The position of the pedestal and of the one photoelectron peak were obtained using the corresponding low light data acquired at this voltage. The number of counts above one quarter photoelectron level in the no-light run was recorded and normalized with respect to the run time to obtain a rate. A typical result is shown in Fig. 5. The (red — online) vertical line denotes the position of the 0.25 photoelectron level. As was the case for the gain, the dark count rate can be used to sort and, if need be, reject tubes based on the particular experimental needs.

The distribution of dark count rates measured in this study is shown in Fig. 6. Tubes that had count rates higher than 5 kHz (about 5.5% of the total) were deemed unsuitable for the GRINCH detector. The cutoff limit is denoted by the vertical (red — online) line in Fig. 6. The "before" and "after" counters keep track of the number of tubes selected based on this criterion.

[2] For this study we prefer the term "dark count rate".

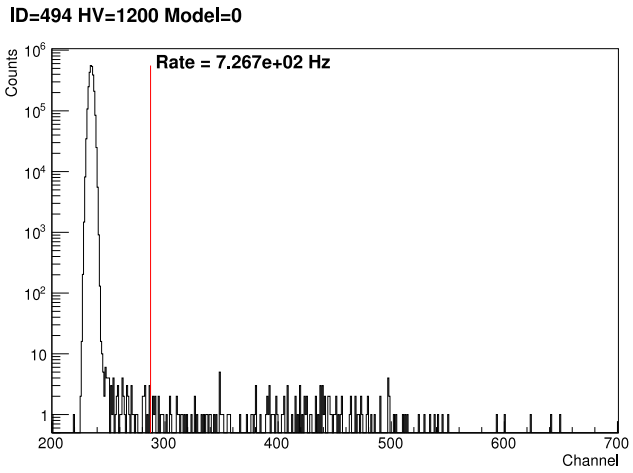

Fig. 5. Dark Count rate for a PMT: Dark count rate measurement for PMT tube # 494. The (red — online) vertical line denotes the position of the 0.25 photoelectron level. (For interpretation of the references to color in this figure legend, the reader is referred to the web version of this article.)

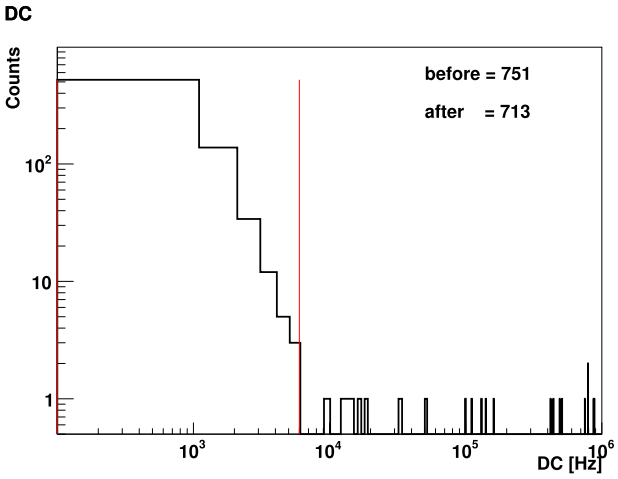

Fig. 6. Dark Count Rate for a batch of tubes: Distribution of dark count rates measured in this study. Tubes with rates higher than 5 kHz were deemed unsuitable for the GRINCH detector. The cutoff limit is denoted by the vertical (red — online) line. (For interpretation of the references to color in this figure legend, the reader is referred to the web version of this article.)

5. Single photoelectron response model comparison

As mentioned in Section 3 several models for the representation of the low light response of a PMT exist. Three of these models were considered in this study. For brevity these were labeled "0" for the Bellamy et al. [7], "1" for the Dossi et al. [6], and "2" for the Degtiarenko model [8].

Fig. 7 shows the three-way comparison between these models when fitted to the same (low light, about 0.1 p.e. per LED pulse) ADC spectrum. The gains calculated using the three models are in good agreement with each other.

This comparison was expanded to the whole set of PMTs tested in this study. Fig. 8 shows the gains obtained using Model 1 (Dossi et al.) versus the gain obtained using Model 0 (Bellamy et al.). The line represents the first diagonal. The relative difference between the gain obtained from an individual model and the weighted average gain is shown in Fig. 9 for all models considered. It can be seen that, for this particular (large) batch of PMTs, the gains obtained using the various models are consistent with each other at the 20% level.

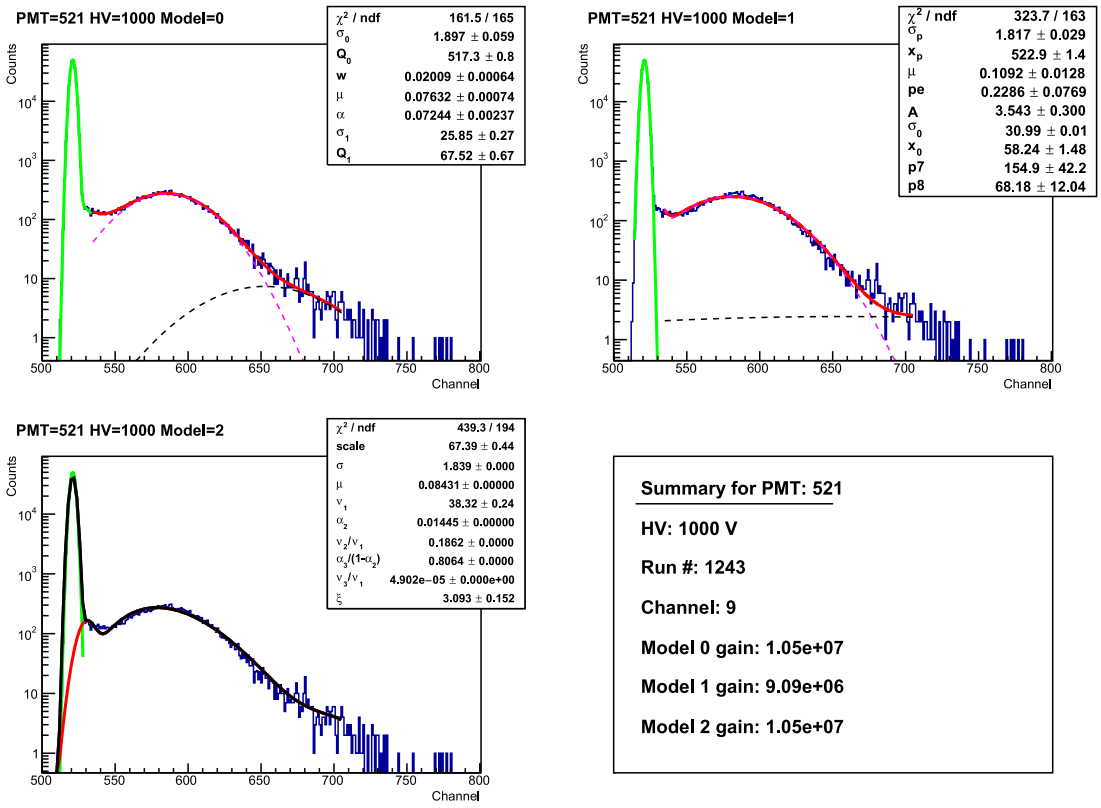

Fig. 7. PMT model comparison for a single tube: Three-way comparison between the PMT signal response models considered in this study.

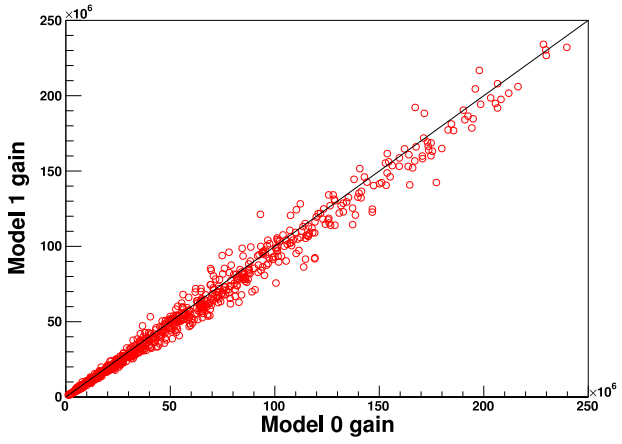

Fig. 8. Two-way model comparison for a batch of tubes: Two dimensional comparison of the gains obtained using two different PMT models for a large batch of tubes. Model labels are as defined in the text.

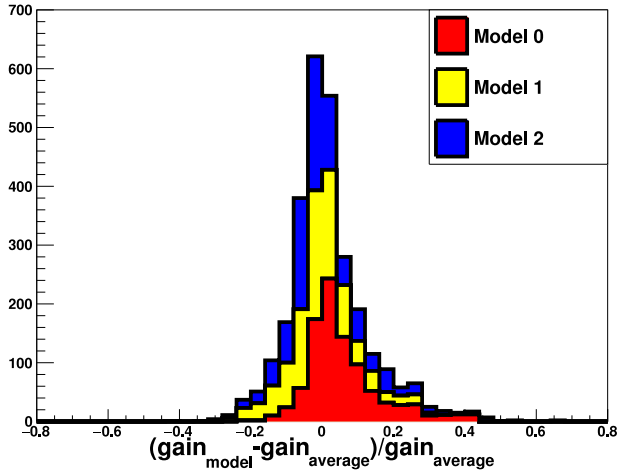

Fig. 9. Three-way model comparison for a batch of tubes: Ratio of the gain residual divided by the average gain for the three different PMT models considered in this study. Model labels are as defined in the text.

Given the shape of the signal all PMT response models considered are highly non-linear, therefore small changes in the starting fit parameters often lead to substantial changes in their output values. To study this effect the main startup parameter (namely the initial guess for the position of the one photoelectron peak) was varied and the fitting procedure was repeated, saving the value of the gain and the χ^2 per degree of freedom. It was observed that for a change of 1 in χ^2/DOF (with respect to the χ^2/DOF of the nominal/best fit) due to change in the startup parameter, the value of the gain can differ by as much as 15%–20%.

Furthermore, due to its nonlinearity the convergence of the fitting procedure is highly dependent on the initial values for the model parameters. As noted in [8] "the stability of the multiparametric fitting procedure strongly depends on the right choice of the parameters' initial value". An often-used solution is to constrain the fit for at least some of its parameters (either by fixing them or by only allowing them to vary in relatively narrow ranges), carry out the fit procedure, save the best values for the parameters, update/expand the range over which parameters can vary, redo the fit. The cycle is then repeated several times. This type of approach can and was automated in our analysis and it produced reasonable results for most PMT spectra. Given the complexity of the functions involved (double summations, convolutions, etc.) and the fact that each spectrum is fitted repeatedly as explained above, even when working with compiled code, as was the case in this analysis, the fitting procedure can be lengthy. For the large

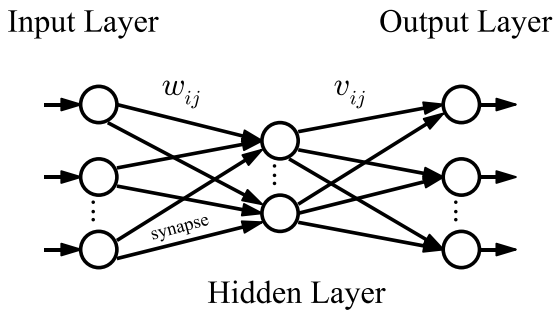

Fig. 10. Typical ANN network: General schematic of a multi layer perceptron network. Only one hidden layer is shown here.

scale testing reported here this automated constrained fitting procedure produced acceptable results for ~80% of the PMT distributions. For the remaining spectra the startup values of the fit parameters had to be interactively assigned. This additional step greatly increased the amount of time required to complete the fit.

6. Artificial neural network based PMT model

Given the difficulties associated with the fitting procedure outlined above alternative ways of obtaining the PMT gain were explored. Ideally, one would want to leverage the results obtained from model-based fits while at the same time avoid some of the pitfalls associated with these. To solve this apparent conundrum an artificial neural network (ANN) was used to model the PMT response.

In this scheme a subset of the PMT spectra were fitted using the models and the result (as "labels") of these fits was used to train the ANN. The results reported here were obtained using the weighted average gain of the three models as the "label". Training with individual model results yielded similar performance. This approach takes full advantage of having a physics-based model while dispensing of the time-consuming need to repeatedly fit problematic spectra. For testing significant number of tubes one can fit a subset of the PMTs to a model, train the neural network, then use the now fixed ANN to obtain the gain for the remaining tubes. This should result in a substantial increase in the analysis speed.

In this study a multi layer perceptron (MLP) type of ANN was used. As shown in Fig. 10 an MLP is a simple feed-forward structure consisting of "neurons" (circles in Fig. 10) interconnected via weighted links called "synapses" (arrows in Fig. 10). Each MLP network has an input layer which accepts the raw data and, optionally, normalizes it, an output layer, and one or more hidden layers. The neurons in each layer are connected with all neurons in the previous as well as the next layer, but are not interconnected among themselves.

The functionality of neurons (other than the input layer which just copies the raw information) can be summarized as follows: the neuron calculates the weighted sum of all of its inputs using the weights associated with each synapse (the set of synapses connecting a layer to the next has a corresponding "weight matrix" associated with it, w_{ij} in Fig. 10) and applies its bias. These value is then used as the input for its "activation" function. For this study this was the so-called "Logistic" or "Sigmoid" function:

$$f(x) = \frac{1}{1 + e^{-x}} \tag{9}$$

In this study the input layer is the full 12 bit QDC spectrum. Even accounting for empty channels this will result in too many input parameters — and correspondingly an unrealistically large number of network weights to be fitted. To reduce the number of inputs (or "features") to a manageable size the following procedure was used: interpreting the raw PMT response as a probability distribution function (PDF) the cumulative distribution function (CDF) was obtained. The CDF was subsequently divided in *q-quantiles* and the positions of the corresponding QDC channels and the original spectrum values at those points were retained as the ANN input values. In this study each spectrum was partitioned in *ventiles* (i.e. 20-quantiles), resulting in 40 inputs for the neural network. Fig. 11 shows four typical PMT spectra and the position of their 20-quantiles (red dots — online). Through further optimization of the ANN the number of the input parameters can be further reduced, though that is beyond the scope of this work.

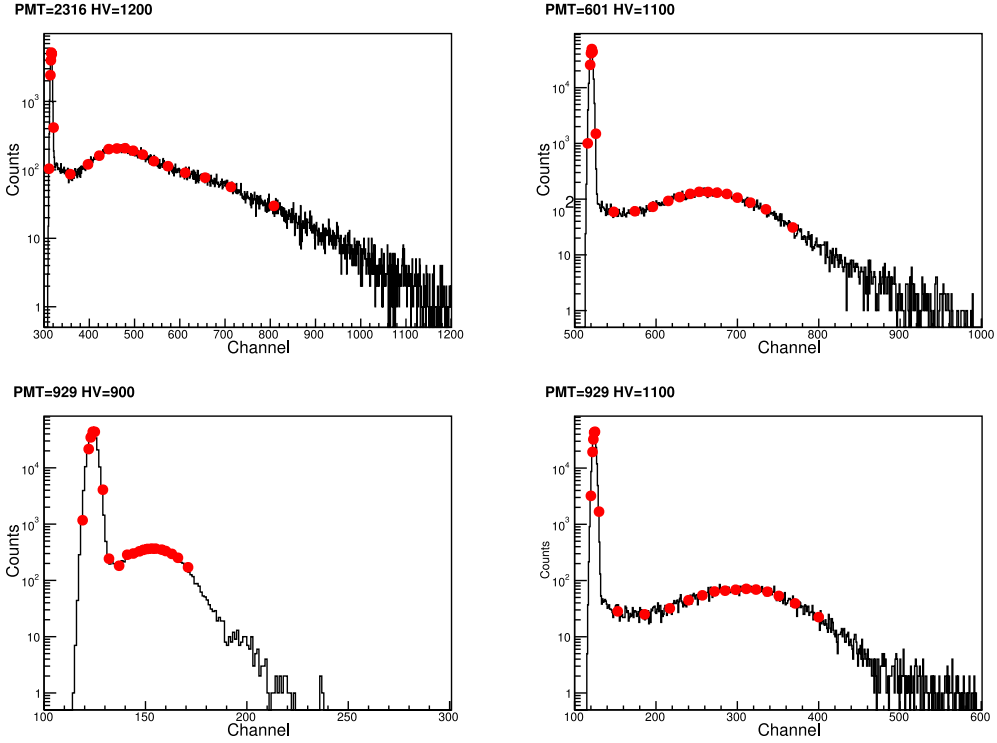

Fig. 11. PMT spectra and the 20-quantiles: Typical PMT spectra and the position of their 20-quantiles (red dots — online).

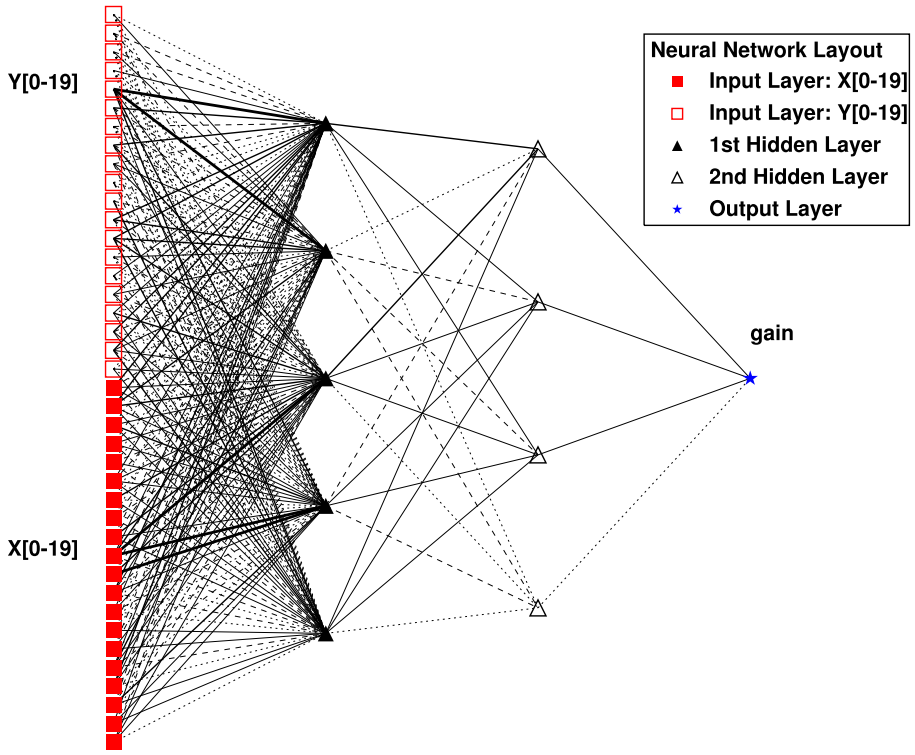

Fig. 12. ANN after training: ANN structure after training. The line thickness is proportional with the weight of that particular synapse.

Using this approach a 40:5:4:1 (two hidden layers with 5 and 4 neurons respectively) ANN was setup and trained using half the available fitted PMT spectra. The remaining spectra were used for testing the results of the ANN after training. Fig. 12 shows the structure of the neural network at the end of the training cycle. The QDC channel numbers are represented with solid squares while the corresponding number of counts are represented using open squares. To improve the efficiency of the training it was useful to normalize both the input values and the output to one. The two hidden layers are represented via solid/open triangles, while the output (in this case the gain) is shown using a star symbol. The line thickness is proportional to the weight associated with that particular synapse. If one were to further optimize this network, a close examination of the weights between the input layer and the first hidden layer and culling the inputs with very low weights would be the obvious starting place.

To test the validity of this approach the ANN was used to evaluate the gain for the PMTs not used for training. Fig. 13 shows the relative difference between the artificial neural network prediction and the model fit. The distribution shows very little bias (~1%–2% level) and its width (~18%) is commensurable with the differences reported earlier between various models considered.

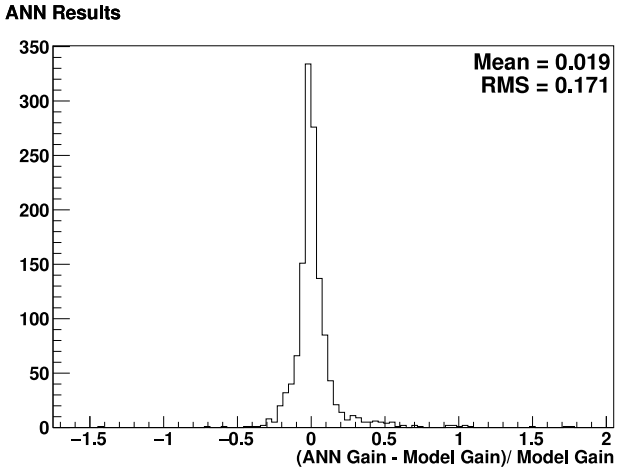

Fig. 13. ANN performance: Relative difference between the ANN and model-based gains, evaluated for the test set only.

7. Conclusion

Results based on the extensive testing of a large (1000+) set of photomultiplier tubes were presented. As these devices will be used in a Cherenkov detector the single photoelectron response, the dark current, and the gain dependence on the tube high voltage were the main measured parameters. Three different phenomenologic parameterizations were implemented in C++ and used to model the low light PMT response. The gains obtained using these three models were shown to be equivalent within the estimated 15%–20 % uncertainties. As these models are highly non-linear they exhibit a very strong dependence on the initial parameters, often requiring time-consuming fine tuning. To address this problem a Machine Learning technique was developed to obtain the gain directly from the raw ADC spectrum: a neural network was trained on a subset of the existing measurements using the average model prediction as labels and the 20th quantile of the raw ADC spectrum as the features. The gain obtained using the neural network was validated on a test set and its performance was similar with the analytic models. While this study is specifically aimed at characterizing tubes for a specific detector (GRINCH) to be used at Jefferson Lab, some of the techniques developed here can be reused for other similar PMT-testing projects.

Acknowledgments

This work was supported by the National Science Foundation Grant # 1307196. The authors thank Todd Averrett, Bogdan Wojtsekhowski, and Pavel Degtiarenko for their interest in our work and useful suggestions. This study would not have been possible without the Jefferson

Lab SBS Collaboration, who welcomed the members of our group in their mix.

References

[1] H. Yao, Technical note for Gas Ring ImagiNg CHerenkov (GRINCH) detector for E 12-06-112, Technical Note, June 2013. See http://wm-jlab.physics.wm.edu/mediawiki/images/5/5d/BGC_Technote.pdf.
[2] I. Adam, et al., Nucl. Instrum. Methods A 538 (2005) 281.
[3] Photomultiplier tubes, Basics and Applications (third ed.), Hamamatsu Corp., 2007. See https://www.hamamatsu.com/resources/pdf/etd/PMT_handbook_v3aE.pdf.
[4] ROOT Data Analysis Framework. See http://root.cern.ch.
[5] JLab Data Acquisition Support. See https://coda.jlab.org/drupal/content/welcome.
[6] R. Dossi, A. Ianni, G. Ranucci, O.Ju. Smirnov, Nucl. Instrum. Methods A 451 (2000) 623.
[7] E.H. Bellamy others, Nucl. Instrum. Methods A 339 (1994) 468.
[8] P. Degtiarenk, Nucl. Instrum. Methods A 872 (2017) 1–15.
[9] Francis J. Lombard, Fred Martin, Statistics of electron multiplication, Rev. Sci. Instrum. 32 (2) (1961) 200–201.